Civil and Environmental Engineering
Vol. 21, Issue 1, 581-590, DOI: 10.2478/cee-2025-0044

PROPOSING CONCRETE MIXTURES FOR MODELS EXAMINED IN SHAKING TABLE TESTS

Ahmed Sabah ALJAWADI[1], Noor S. TARESH[2], Malik H. ASSI[3, *], Sophia C. ALIH[4]

[1] Fediral commission of Integrity, Engineering Department, Baghdad, Iraq
[2] Department of Highways and Transportation Engineering, College of Engineering, Mustansiriyah University, Baghdad, Iraq
[3] Department of Water Resources Engineering, College of Engineering, Mustansiriyah University, Baghdad, Iraq
[4] Institute of Noise and Vibration, Faculty of Civil Engineering, Universiti Teknologi Malaysia, Johor, Malaysia
[*] corresponding author: malik_habeeb@uomustansiriyah.edu.iq

Abstract

This paper focuses on the development of micro-concrete mixes used to construct scaled model buildings which needs to be examined by the shaking table test to simulate the key strength and stiffness characteristics of full-scale model. Eighteen trial mixes have been derived from a normal concrete mix to achieve this study. Owing to the vital importance of aggregate type and gradation in achieving appropriately low strength concrete, mixes were developed by replacing a specific portion of coarse aggregate with crushed rubber or crushed glass. In addition to the aggregate replacement, water-cement ratios for other mixes were increased as well. The mechanical properties of these developed micro-concrete mixes have been obtained to provide extensive information concerning the validity of using them for distorted scaled model.

Keywords:
Micro-concrete;
Shaking table;
Coarse aggregate;
Crushed rubber;
Crushed glass.

1 Introduction

Associating earthquake requirements to structural capacity requires the capacity to be examined under circumstances closely resembling the dynamic conditions of the actual structure [1]. The shaking table test is a key approach to examining the structural behaviour and failure mechanisms of structures under such seismic loading conditions. These can be isolated structures, residential buildings, hydraulic structures and structures equipped with energy dissipation devices [2]. Since the sixties, the test has been used in evaluating both the seismic and dynamic responses of civil engineering structures [3]. On the other hand, laboratories equipped with extremely high-load capacity facilities are required if the dynamic structural response of full-scale concrete structures under seismic loading conditions is to be evaluated. Due to the limitations of such specialized laboratories and the high cost associated with both the use and getting rid of the examined specimens, engineers turn to employ scaled models to predict the prototype behaviour. At specific geometric scale factors, these scaled-down structural models represent a smart way to conduct dynamic loading experiments with minimal cost. The shaking table test using a scaled structure model is one of the most operative means to investigate buildings after taking into account the practical, economic and accurate sides of the experiments [4, 5]. The ideal scaled model can be achieved when it is geometrically like the prototype and utilize same materials of prototype, this model called “replica model”. If the model simulates the entire behaviour of the structural system as it is being loaded to failure, precise replication of the prototype concrete characteristic is essential. Owing to technical and physical reasons, it is sometimes unattainable to produce the replica model. Consequently, materials change and/or some deviations in the dimensions may occur during scale models’ construction. Models that are geometrically undistorted, compared with prototype, but constructed by utilizing different materials are termed dissimilar material model. Although replica is considered the most appropriate model, reaching a perfect match with full scale structures is difficult, making dissimilar material scale model the best alternative.

It is straight forward to derive the basic similitude relation from the dynamic equation i.e., $E_r /(g_r \rho_r) = l_r$. Where, E_r, l_r, ρ_r and g_r indicate the similitude ratios of modulus elasticity, length, density and gravity acceleration, respectively. If the gravity acceleration g is not changed, and it should not be, then the equation becomes $E_r = l_r \rho_r$. From the equation, it is deduced that similar materials can be used for both the full and scaled model if and only if the length ratio is unity. If the ratio is to be less than one, a material that is comparably heavier, less stiff or both must be used in the scaled model to provide concrete properties that will be appropriate with the similitude laws and the shaking table capacity.

Selecting the model concrete is regarded as one of the most problematic steps in the construction process of a small-scale model. In general, four properties with specific values under short-term load must be possessed by a model concrete: ultimate compressive strength, ultimate compressive strain, secant modulus of elasticity and ultimate tensile strength [6, 7]. Various studies using micro-concrete have shown that satisfactory results can be attained if it is controlled properly [8-14]. In these studies, scaled-down models have strength smaller than the concrete strength of prototype to overcome the limitation of shaking table capacity. Nonetheless, neither mix proportions nor mix selection mechanisms are clarified in detail. This could be attributed to the minimal strength reductions needed in their work. It is worth mentioning that occasionally there is a need to achieve high reduction of strength to meet the similitude requirements. Besides, referring to the similitude relation above, it is obvious that the mass is directly proportional to strength.

It has been shown that the characteristics of concrete change when automobile tyre chips are added to the concrete mix. The compressive strength and modulus of elasticity of normal concrete is greater than that of rubberized concrete. The rate of strength reduction relies on the amount of rubber particles added to concrete [15-17]. It has been reported that rubberized concrete members possess higher deformability or ductility compared to those members made out of made from normal concrete [18-21]. Furthermore, in rubberized concrete, the modulus of elasticity and strength are indirectly proportional to the rubber content. The values of brittleness index of rubberized concrete are smaller than that of normal concrete, meaning that rubberized concrete has higher ductility performance in comparison to normal concrete [22].

The replacement of crushed glass with one or more of the concrete compositions will also lead to a decrease in concrete strength. Glass is vulnerable to chemical attack under high alkali conditions, resulting from cement hydration in concrete. This is attributed to its amorphous structure and silica-rich nature. This chemical attack possibly produces changed extensive formation of ASR gel. The gel is expansive and may lead to premature cracking in the concrete if suitable precautions are not taken in the preparation of the concrete mix [23]. Consequently, low-strength concrete could be produced by replacing one of the concrete mix components by certain proportions of waste crushed glass. Terro [24] investigated the crushed glass replacement effect on the compressive strength of concrete within a range from 0% up to 100% of aggregate, the crushed glass of bottles was replaced with coarse aggregate, fine aggregate, coarse and fine aggregate. The result showed that the strength of concrete for all types of replacements started to decrease for the percentage beyond 25% of aggregate replacement. Ali & Al-Tersawy [25] stated that replacing fine aggregates with crushed waste glass (CWG) results in lower modulus of elasticity values. Moreover, increasing CWG replacement ratio brings about a reduction in the concrete modulus of elasticity [26]. Likewise, [27] showed that CWG content up to 20% has no effect on the modulus of elasticity of concrete. Conversely, higher replacement levels lead to a decrease in the modulus of elasticity.

A series of low-strength mixes has been developed herein to provide alternative choices of normal micro-concrete. These substitutes can possibly be used as a reference for researchers whenever facing the carrying weight limitations of test instruments. Owing to the vital importance of aggregate type and gradation in achieving appropriately low-strength concrete, mixes were developed by replacing a specific portion of coarse aggregate with crushed rubber or crushed glass. In addition to the aggregate replacement, water-cement ratios for other mixes were increased as well. The compressive strength, tensile strength, modulus of elasticity and stress-strain curves of these developed micro-concrete mixes have been obtained to provide extensive information concerning the validity of using them for distorted scaled model.

2 Experimental works

2.1 Concrete mixes

Being a heterogeneous material makes it difficult to simulate concrete. This is due to the complexity of the numerous factors that affect the characteristics of the hardened concrete. Theoretically, aggregate size, pores size in the gel and voids size of the hardened concrete are all required to be scaled. While some of the above requirements are partially satisfied because of using small-size aggregate, cement particles cannot be scaled. In other words, it is impossible to produce a precise simulation of a small-scale model concrete [6]. Hence, the selection of model materials herein was done based on a practical (not theoretical) basis. The control mix developed from existing data of micro-concrete was conducted earlier at the University Technology Malaysia. After conducting several trial mixes, the control micro-concrete mix was designed to have a strength of 30 MPa at 28 days according to the British standards BS5328: Part 2: 1997 [28]. The first micro-concrete control mix (MCI) has a water/cement ratio of 0.42, 550 kg/m3 of ordinary Portland cement, 233 kg/m3 of fresh water, 511 kg/m3 of fine aggregate and 1086 kg/m3 of coarse aggregate. The fine aggregate was washed river sand, passing from a sieve 2mm, and the particle size of the coarse aggregate ranged from 3 to 5 mm. The drive behind choosing such aggregate sizes was to allow even distribution of fresh concrete in congested reinforcement. To enhance both the mixture's workability and early hardening strength, 6.6 kg/m3 (1.2% of cement powder) superplasticizer was added to the control micro concert mix. The second micro-concrete control mix, MCII, was produced by reducing the amount of control mix cement by 50%. The new mixes developed from the control mixes by replacing a specific percentage of coarse aggregate with either crushed rubber with a maximum particles size of 5mm or crushed glass with a maximum particles size of 4mm (see Fig. 1). These mixes were used to cast the test cylinders and are shown in Table 1 and Table 2.

Fig. 1: Course materials (Left) aggregate (middle) crushed rubber (Right) crushed glass.

Table 1: Micro-Concrete I and the driven mixes.

Mix	Cement (kg)	Water (kg)	Sand model (kg)	Gravel model (kg)	Material (kg)
MCI	550	233	511	1086	/
RMI					**Rubber**
RM I (10%)	550	233	511	977.4	108.6
RM I (20%)	550	233	511	868.8	217.2
RM I (30%)	550	233	511	760.2	325.8
RM I (40%)	550	233	511	651.6	434.4
RM I (50%)	550	233	511	543	543
CGM I					**CG**
CGM I (25%)	550	233	511	814.5	271.5
CGM I (50%)	550	233	511	543	543
CGM I (75%)	550	233	511	271.5	814.5

Table 2: Micro-concrete II and the driven mixes.

Mix	Cement (kg)	Water (kg)	Sand model (kg)	Gravel model (kg)	Material (kg)
MCII	275	233	511	1086	/
RM II					**Rubber**
RM II (10%)	275	233	511	977.4	108.6
RM II (20%)	275	233	511	868.8	217.2
RM II (30%)	275	233	511	760.2	325.8
RM II (40%)	275	233	511	651.6	434.4
RM II (50%)	275	233	511	543	543
CGM II					**CG**
CGM II (25%)	275	233	511	814.5	271.5
CGM II (50%)	275	233	511	543	543
CGM II (75%)	275	233	511	271.5	814.5

2.2 Cylinders preparation and casting

For each mix batch, 15 test cylinders were made: 6 for compressive tests, 6 for split tensile tests and 3 for stress-strain curve and Young's modulus calculations. The cylinders used in the test were made according to ACI Committee 444 (1979) with recommended dimensions of 50×100 mm (2×4 in) and accepted as a standard for comparing different model micro-concrete mixes (Noor and Boswell, 1992). For each mix shown in Tables 1 and 2, the dried constituents were mixed well manually using a small shovel and then the water and the admixture were added to the mix. The mixing was stopped after reaching uniform consistency. The mix was poured into PVC cylindrical moulds, which were prepared in advance. The cylinders were then filled in three layers, each new layer compacted by 25 strokes of a 12 mm rod. After smoothing the upper surface of the concrete, the moulds were left undisturbed for 24-48 hours depending on the mix type (see Fig. 2). Subsequently, the moulds were stripped, and the specimens were transferred to the water tank and kept immersed in water until about 1 hour before the beginning of the actual test, then each sample have been weighed to calculate the average density of each mix. To ensure constant temperature of 24 ± 2 °C, the water tanks was placed inside the laboratory until the test.

Fig. 2: Micro-concrete cylinders casting.

3.3 Instrumentation and loading

3.3.1 Compressive strength test

The compressive strength test was conducted in accordance with BS EN 12390-3:2009 [29]. Prior to testing, the samples were prepared, and the surface area of the concrete was elevated by grinding using a hand flat fill tool. A typical compressive strength testing machine was used to carry out the tests. A constant loading rate of 0.6 MPa per second was selected and applied until the failure of the specimen. See Figure 3. Despite being automatically generated by the machine, the following equation was used as well as to validate the tests' outcomes:

$$f_{ck} = F/Ac \quad (1)$$

where:
f_{ck} = the compressive strength, in (MPa), F = the maximum load at failure, in (N) and Ac = the cross-sectional area of the specimen, in (mm^2).

Fig. 3: Compressive strength test (left) prepared cylinders (right) testing machine.

3.3.2 Tensile splitting strength

An indirect tensile strength test was carried out in accordance with BS EN 12390-6:2009 [29]. Cylindrical-shaped test samples compliant with BS EN 12390-6:2009 were used in this test. A constant rate of stress within the range of 0.05 MPa/s was selected and applied until the specimen was split into two hemispheres. Fig. 4 shows the splitting tensile strength testing. The following equation was used to calculate the tensile splitting strength:

$$f_{st} = \frac{2F}{\pi L d} \quad (2)$$

where:
f_{st} = tensile splitting strength, in (MPa), F = maximum load at failure, in (N), L = length of the specimen, in (mm), d = cross-sectional dimension, in (mm).

Fig. 4. Splitting tensile strength test.

3.3.3 Modulus of elasticity

This part deals with the deformation of concrete specimens under compressive loads to determine the elastic behaviour of Normal micro-concrete, rubberized micro-concrete and crushed glass micro-concrete. The modulus of elasticity (E) is mathematically determined as the gradient of the line in the reversible region of a stress-strain curve. The modulus of elasticity is significantly used in structural design. In fact, it represents the maximum allowable stress, before the material goes to the plastic zone, which is identified as permanent deformation. The elastic modulus of the materials determines the rigidity of the design structure. However, due to the nonlinearity of the strain-stress curve, the three types of modulus are defined using three methods. The “tangent modulus” is defined by the gradient of a tangent to the stress-strain curve, at whichever point on the curve. The second type of modulus of elasticity is “chord modulus.” The “secant modulus” is defined by the gradient of a line drawn from the origin to the point corresponding to 33% of ultimate strength according to BS 8110: Part 2 [30]. The secant modulus of elasticity was computed in accordance with BS 8110: Part 2 [30].

Measuring strains in compressed concrete cylinders is a main difficulty. Glued strain gages extract only local information which may become pointless if a crack develops under the gage. Furthermore, this method is unproductive in studies in which a large number of samples is to be examined, owing to the high cost and large amount of preliminary work involved [31].

Therefore, an omega gauge (Pi-type displacement transducer) with a length equal to half the test cylinder height was installed to measure the strain in the test cylinder (see Figure 5) [32]. Furthermore, three samples were tested to insure reliability. The data logger, which was connected to the computer, monitored and recorded the applied load and their corresponding strain. The obtained modulus of elasticity is the average of three samples, where each sample was obtained using three cycling load processes. For each sample, a loading of up to one-third of ultimate load was applied, and then, the unloading was done at the same pace. Finally, the modulus of elasticity values was computed by using the following equation:

$$\boldsymbol{E} = \frac{\Delta\sigma}{\Delta\varepsilon} \quad (3)$$

where:
Δσ: the variance in stress between a basic loading of 0.5 N/mm2 a higher loading level of 1/3 of the compressive strength of the micro-concrete,
Δε: the variance in strain between a basic loading of 0.5 N/mm2 an upper loading level of 1/3 of the compressive strength of the micro-concrete.

Fig. 5. Stress-strain test.

4 Density of micro-concrete

The density for all mixes at 28-day curing ages is shown in Tables 3, 4 and 5. The results reveal the decreasing tendency of the hardened density as the crushed glass ratio increases in comparison with controlled mixes. This is due to the lower density of glass aggregate if compared to that of natural sand. The density of MCI decreased by 1.5%, 3% and 4% for 25%, 50% and 75% glass replacement respectively. While the reduction of micro-concrete II density was 1.2%, 1.7% and 3% for 25%, 50% and 75% glass replacement respectively.

Regarding the replacement of Rubber, it is found that decreasing in density is higher than glass reduction where, the density was observed to be 5%, 8%, 14%, 17% and 19% for 10%, 20%, 30%, 40%

and 50% respectively for rubber replacement in MCI. It can also be observed that the reduction percent in the density of MCII due to the rubber replacement were 8%, 10%, 17%, 22% and 23% for 10%, 20%, 30%, 40% and 50% respectively. The high reduction percent of density is a result of low density of rubber.

Table 3: Summary of micro-concrete cylinder tests.

Mix		***Micro-concrete I***	***Micro-concrete II***
Density (kg/m^3)		2365	2234
f_{ck} (avg.)	*7 Days*	35.5	13.1
	28 Days	37	17.3
fst (avg .)	*7 Days*	2.2	1.7
	28 Days	4	2.6
E (Gpa)		22.9	12.7
ε @ f_{ck} mm/mm		0.0024	0.0029
f_{st}/f_{ck}	*7 Days*	0.06	0.13
	28 Days	0.11	0.15

5.2 Rubberized micro-concrete

Table 4 shows the results obtained from testing cylinders of control mix I and (RMI and RMII). Compared to the Micro-concrete I, Table 4 shows that the strain of RM I mixes at maximum stress was increased where the strain was significantly increased with the increment of Rubber amount replacement. RMI mixes were much softer, as indicated by E in Table 4 and Fig. 6. The average split tensile strength was decreased. In terms of the ratio of fst to fck, RM I had a higher ratio than the control specimen while, RMI mixes had a tensile strength lower than the micro-concrete I.

On the other hand, the control mix II and RMII properties results which are obtained from the same sized cylinders mentioned above are shown in Table 4. The data show that the compressive strength, splitting tensile strength test, and modulus of elasticity of control mix II were decreased when the coarse aggregate was replaced with rubber. The value of strength relatively decreased with the increasing of rubber proportion replacement of coarse aggregate. However, the fst to fck ratio of RMII was higher than control mix II.

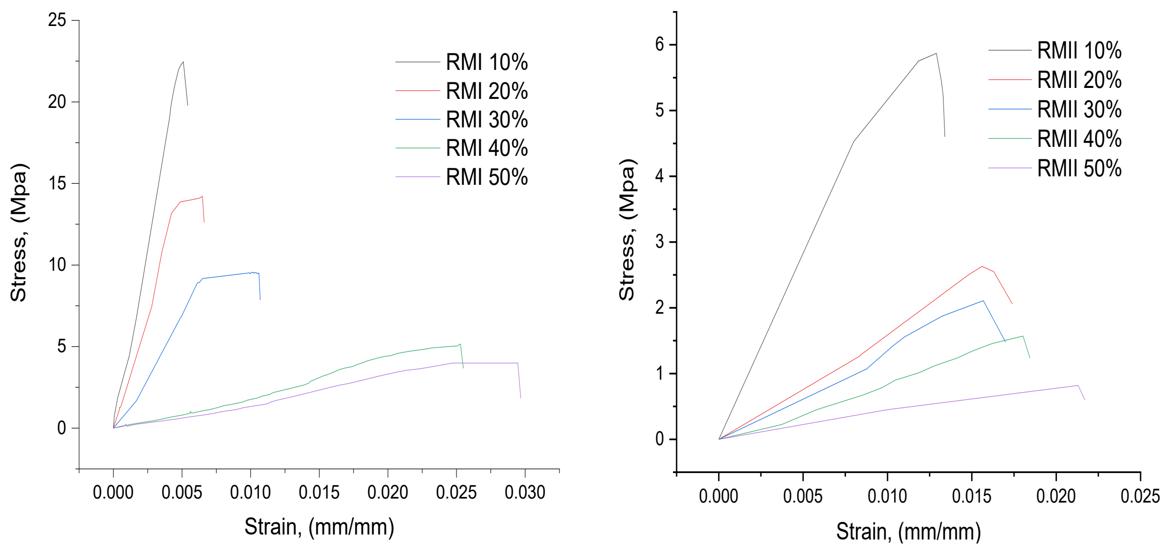

Fig. 6 Stress-strain curves of (a) RM I mixes, (b) RM II mixes.

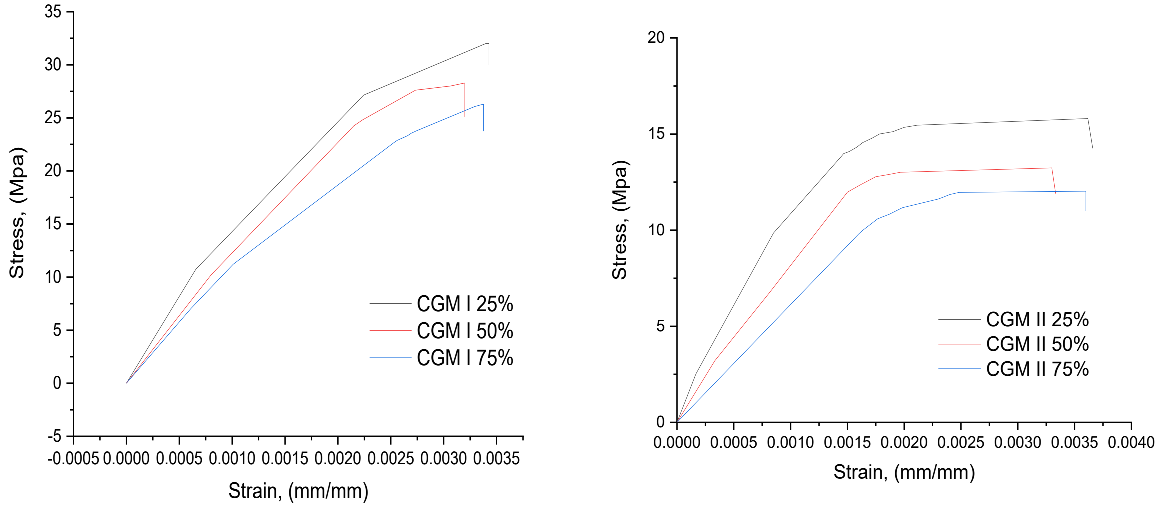

Fig. 7: Stress-strain curves of (a) CGM I mixes (b) CGM II mixes.

5.3 Crushed glass micro-concrete

The compressive stress-strain curves and basic properties of crushed glass micro-concrete are presented in Fig. 7and Table 5 respectively. The average split compressive strength and tensile strength of CGM mixes were decreased compared to the normal micro-concrete when the glass was used for coarse aggregate replacement. The ratio of fst/fck CGMI is same to that for Micro-concrete I, while the ratio was increased for the CGMII.

Table 4: Summary of rubberized micro-concrete cylinder tests.

Mix	***Density (kg/m³)***	***fck (avg.)***		***fst (avg .)***		***E (Gpa)***	***ε @ fck mm/mm***	***fst/fck***	
		7 Days	***28 Days***	***7 Days***	***28 Days***			***7 Days***	***28 Days***
Microconcrete I	2365	35.5	37.0	2.2	4.0	22.9	0.0024	0.06	0.11
RM I 10%	2243	15.4	21.3	1.9	2.8	6.1	0.0053	0.12	0.13
RM I 20%	2170	13.9	15.1	1.8	1.9	5.5	0.0065	0.13	0.13
RM I 30%	2025	9.1	10.1	1.7	1.3	2.3	0.0098	0.19	0.13
RM I 40%	1962	5.1	6.4	1.1	1.3	0.8	0.0252	0.22	0.20
RM I 50%	1910	4.5	4.1	0.8	1.0	0.5	0.0297	0.19	0.25
Microconcrete II	2234	13.1	17.3	1.7	2.6	12.7	0.0029	0.13	0.15
RM II 10%	2052	6.6	7.6	1.1	1.4	6.8	0.0129	0.17	0.19
RM II 20%	2009	3.3	3.8	0.8	0.9	4.1	0.0156	0.25	0.23
RM II 30%	1847	1.7	2.1	0.5	0.6	1.3	0.0157	0.27	0.27
RM II 40%	1741	1.0	1.0	0.2	0.3	0.5	0.0182	0.16	0.27
RM II 50%	1720	0.8	0.8	0.2	0.3	0.3	0.0213	0.23	0.37

Table 5: Summary of crushed glass microconcrete cylinder tests.

Mix	***Density (kg/m3)***	***fck (avg.)***		***fst (avg .)***		***E (Gpa)***	***ε @ fck mm/mm***	***fst/fck***	
		7 Days	***28 Days***	***7 Days***	***28 Days***			***7 Days***	***28 Days***
Micro-concreteI	2365	35.5	37.0	2.2	4.0	22.9	0.0024	0.06	0.11
CGMI 25%	2329	30.3	33.5	2.4	3.6	20.2	0.0033	0.08	0.11
CGMI 50%	2296	26.9	27.3	1.9	3.4	18.8	0.0032	0.07	0.12
CGMI 75%	2269	23.8	25.2	1.9	3.0	14.3	0.0034	0.08	0.12
Micro-concreteII	2234	13.1	17.3	1.7	2.6	12.7	0.0029	0.13	0.15
CGMII 25%	2207	9.3	10.1	1.6	2.2	10.8	0.0036	0.18	0.22
CGMII 50%	2197	7.3	8.1	1.3	1.8	8.1	0.0033	0.18	0.22
CGMII 75%	2166	6.6	6.2	1.0	1.3	6.2	0.0037	0.16	0.21

5.3 Crushed glass micro-concrete

The compressive stress-strain curves and basic properties of crushed glass micro-concrete are presented in Fig. 8 and Table 5 respectively. The average split compressive strength and tensile strength of CGM mixes were decreased compared to the normal micro-concrete when the glass was used for coarse aggregate replacement. The ratio of fst/fck CGMI is same to that for Micro-concrete I, while the ratio was increased for the CGMII.

6 Conclusion

The data presented in this paper concluded that by reducing the cement content of the normal micro-concrete mix to the half, the compressive strength, splitting tensile strength and modulus of elasticity were reduced by about 50% and the ultimate compressive strain was slightly increased. On the other hand, the replacing of the coarse aggregate with crushed rubber reduces the compressive strength, splitting tensile strength, and modulus of elasticity of normal micro-concrete, and this reduction was increasing simultaneously with the increasing the replacement proportion while the ultimate compressive strain becomes higher. The glass replacement produced a low reduction in the compressive strength, tensile strength and Young's modulus compared to the rubber replacement. Furthermore, it is showed a slight reduction in the density of micro-concrete in comparison with the rubber replacement.

References

[1] A. DERECHO, M. IQBAL, M. FINTEL, AND W. CORLEY, "Loading history for use in quasi-static simulated earthquake loading tests," *Special Publication,* vol. 63, pp. 329-356, 1980.

[2] X. LU, Q. LU, W. LU, Y. ZHOU, AND B. ZHAO, "Shaking table test of a four-tower high-rise connected with an isolated sky corridor," *Structural Control and Health Monitoring,* vol. 25, no. 3, p. e2109, 2018.

[3] P. B. LOURENÇO, L. AVILA, G. VASCONCELOS, J. P. P. ALVES, N. MENDES, AND A. C. COSTA, "Experimental investigation on the seismic performance of masonry buildings using shaking table testing," *Bulletin of Earthquake Engineering,* vol. 11, pp. 1157-1190, 2013.

[4] X. LU, Y. ZHOU, AND W. LU, "Shaking table model test and numerical analysis of a complex high-rise building," *The Structural Design of Tall and Special Buildings,* vol. 16, no. 2, pp. 131-164, 2007.

[5] J. M. LIROLA, E. CASTAÑEDA, B. LAURET, AND M. KHAYET, "A review on experimental research using scale models for buildings: Application and methodologies," *Energy and Buildings,* vol. 142, pp. 72-110, 2017.

[6] W. KIM, A. EL-ATTAR, AND R. N. WHITE, *Small-scale modeling techniques for reinforced concrete structures subjected to seismic loads*. National Center for Earthquake Engineering Research, 1988.

[7] H. G. HARRIS AND G. SABNIS, *Structural modeling and experimental techniques*. CRC press, 1999.

[8] W. XU, W. YANG, C. ZHANG, AND D. YU, "Shake Table Test for the Collapse Investigation of a Typical Multi-Story Reinforced Concrete Frame Structure in the Meizoseismal Area," *Applied Sciences,* vol. 7, no. 6, 2017.

[9] W. XU, J. SUN, W. YANG, AND K. DU, "Shaking table comparative test and associated study of a stepped wall-frame structure," *Earthquake Engineering and Engineering Vibration,* vol. 13, no. 3, pp. 471-485, 2014.

[10] Z. XIONG, X. CHEN, C. ZHANG, X. HUO, AND Y. ZHUGE, "Shaking table tests of RC frame structure across the earth fissure under earthquake," *The Structural Design of Tall and Special Buildings,* vol. 27, no. 14, 2018.

[11] X. LU, Q. LU, W. LU, Y. ZHOU, AND B. ZHAO, "Shaking table test of a four-tower high-rise connected with an isolated sky corridor," *Structural Control and Health Monitoring,* vol. 25, no. 3, 2018.

[12] X. LU, Y. ZOU, W. LU, AND B. ZHAO, "Shaking table model test on Shanghai World Financial Center Tower," *Earthquake Engineering & Structural Dynamics,* vol. 36, no. 4, pp. 439-457, 2007.

[13] X. LU, Y. ZHOU, AND W. LU, "Shaking table model test and numerical analysis of a complex high-rise building," *The Structural Design of Tall and Special Buildings,* vol. 16, no. 2, pp. 131-164, 2007.

[14] C. LI, S. LAM, M. ZHANG, AND Y. WONG, "Shaking table test of a 1: 20 scale high-rise building with a transfer plate system," *Journal of structural engineering,* vol. 132, no. 11, pp. 1732-1744, 2006.

[15] S. AHMED, A. ALMUTAIRI AND W. DOMAT, "Non-Linear analysis of Hybrid reinforced T-beam with partial substitution recycled rubberized concrete," *Civil and Environmental Engineering,* vol. 20, no 1, pp. 397-410, 2024.
[16] Z. MARCALIKOVA, R. GANDEL, J. JERABEK AND J. VARAK "Selected properties and microstructure of concrete with tire rubber granulate as recycled material in construction industry," *Civil and Environmental Engineering,* vol. 20, no 2, pp. 754-766, 2024.
[17] M. ASSI AND N. TARESH, "Punching shear strength of flat slabs strengthened with internal flexible CFRP pateches," IOP Conf. Series: Materials Science and Engineering 737 (2020) doi:10.1088/1757-899X/737/1/012009.
[18] I. B. TOPCU, "The properties of rubberized concretes," *Cement and concrete research,* vol. 25, no. 2, pp. 304-310, 1995.
[19] I. B. TOPÇU AND N. AVCULAR, "Collision behaviours of rubberized concrete," *Cement and Concrete Research,* vol. 27, no. 12, pp. 1893-1898, 1997.
[20] H. A. TOUTANJI, "The use of rubber tire particles in concrete to replace mineral aggregates," *Cement and Concrete Composites,* vol. 18, no. 2, pp. 135-139, 1996.
[21] N. N. ELDIN AND A. B. SENOUCI, "Rubber-tire particles as concrete aggregate," *Journal of materials in civil engineering,* vol. 5, no. 4, pp. 478-496, 1993.
[22] L. ZHENG, X. S. HUO, AND Y. YUAN, "Strength, modulus of elasticity, and brittleness index of rubberized concrete," *Journal of Materials in Civil Engineering,* vol. 20, no. 11, pp. 692-699, 2008.
[23] A. SHAYAN, "Value-added utilisation of waste glass in concrete," in *IABSE Symposium Report*, 2002, vol. 86, no. 6, pp. 12-21: International Association for Bridge and Structural Engineering.
[24] M. J. TERRO, "Properties of concrete made with recycled crushed glass at elevated temperatures," *Building and environment,* vol. 41, no. 5, pp. 633-639, 2006.
[25] E. E. ALI AND S. H. AL-TERSAWY, "Recycled glass as a partial replacement for fine aggregate in self compacting concrete," *Construction and Building Materials,* vol. 35, pp. 785-791, 2012.
[26] H.-Y. WANG, "A study of the effects of LCD glass sand on the properties of concrete," *Waste Management,* vol. 29, no. 1, pp. 335-341, 2009.
[27] M. C. LIMBACHIYA, "Bulk engineering and durability properties of washed glass sand concrete," *Construction and Building Materials,* vol. 23, no. 2, pp. 1078-1083, 2009.
[28] *Method of Specifying Concrete Mixes*, 1997.
[29] B. EN, "12390-6 2009 Testing hardened concrete, Part 6: tensile splitting strength of test specimens," *British Standards Institution,* 2009.
[30] B. Standard, "Structural use of Concrete–Part 2: Code of practice for special circumstances," *Reprinted incorporating amendments Nos. 1 and,* vol. 2, pp. 8110-2, 1985.
[31] P. D. MONCARZ AND H. KRAWINKLER, *Theory and application of experimental model analysis in earthquake engineering*. Stanford University California, 1981.
[32] A. KAMAL, M. KUNIEDA, N. UEDA, AND H. NAKAMURA, "Evaluation of crack opening performance of a repair material with strain hardening behavior," *Cement and Concrete Composites,* vol. 30, no. 10, pp. 863-871, 2008.
[33] R. SHARMA, F.-P. HSIAO, K.-Y. LIU, AND C. E. PON, "Shaking table test of a half-scale three-story non-ductile RC building subjected to near-fault ground motions: Experimental and numerical modeling," in *Structures*, 2022, vol. 45, pp. 721-747: Elsevier.
[34] J. IYAMA, C. C. OU, S. YAMADA, K. CHIBA, AND M. TOYOSHIMA, "Shaking table test of steel truss frame focusing on acceleration and strain response for post-earthquake buckling evaluation," *Bulletin of Earthquake Engineering,* vol. 21, no. 5, pp. 2759-2783, 2023.
[35] S. SAHOO, B. MANNA, AND K. SHARMA, "Shaking table tests to evaluate the seismic performance of soil nailing stabilized embankments," *International Journal of Geomechanics,* vol. 21, no. 4, p. 04021036, 2021.